International Symposium
Non-Destructive Testing in Civil Engineering (NDT-CE)

September 15 - 17, 2015, Berlin, Germany

A comparison of TSD, FWD and GPR field measurements

Wayne B. MULLER [1,2,3]

[1]Department of Transport and Main Roads
Brisbane, Queensland, Australia; Phone: +61 7 32603510; Fax: +61 730663011;
e-mail: wayne.b.muller@tmr.qld.gov.au;
[2]ARRB Group Ltd
Brisbane, Queensland, Australia
[3]School of Civil Engineering, The University of Queensland
Brisbane, Queensland, Australia

Abstract

The combined use of Traffic Speed Deflectometer (TSD) and Noise-Modulated Ground Penetrating Radar (NM-GPR) technologies shows significant potential for rapid non-destructive investigation of road pavements. This paper presents a summary of recent field investigations using these devices and conventional Falling Weight Deflectometer (FWD) in combination. Geospatial views of the data were developed to enable easier alignment, comparisons and better understanding of the road condition, by viewing these complementary data together and in the context of the surrounding environment. Similarities and differences between these measurements and an overview of the potential use of these techniques in combination are also discussed.

Keywords: Traffic Speed Deflectometer (TSD), Ground Penetrating Radar (GPR), Falling Weight Deflectometer (FWD), rapid pavement investigations

1. Introduction

In recent years the Traffic Speed Deflectometer (TSD) has emerged as a device with significant potential for rapid non-destructive investigation of road pavement structural response [1-3]. To enable better understanding and use of TSD measurements, knowledge of the pavement structure is also required. Noise-Modulated Ground Penetrating Radar (NM-GPR) is an emerging technology that enables rapid and non-destructive measurement of 'as constructed' pavement layering information. This technology can be used to determine pavement layering information where unknown, or to check the accuracy of existing records [4]. During 2010, a comparison of first-generation TSD and NM-GPR measurements was undertaken, finding the methods were complementary and highlighting the potential of using these technologies in combination [5]. Since that time both TSD and the NM-GPR technologies have been further developed. This paper reports on a recent trial comparing measurements using updated versions of TSD and NM-GPR technologies along with conventional Falling Weight Deflectometer (FWD) measurements. The comparisons are presented visually using Google Earth™ software, enabling the collected data to be better understood by being viewed in the context of the local environment.

2. Technology and initial work

2.1 Traffic Speed Deflectometer (TSD)

Developed by Greenwood Engineering, the TSD is a semi-trailer device that employs a series of Doppler-shift lasers within a rigid instrumented frame to determine the velocity and slope of the deflecting road surface at discrete points ahead of a loaded rear wheel [6]. The deflection profile of the road surface can then be determined either by curve fitting and numerical integration [6] or by fitting pavement or empirical models to these measurements [7-9].

In 2010 a first-generation TSD device was trialled in the Australian states of Queensland and New South Wales [1, 2, 10]. Those investigations reported repeatable deflection slope measurements for a range of collection speeds and other conditions. Later re-analysis of the Queensland data using a simplified approach improved the analysis, producing deflection results much closer to that reported by FWD [6]. The success of the 2010 initial investigations led to the establishment of a 5-year program of TSD investigations for the road authorities of Queensland, New South Wales and New Zealand.

In 2014, a second generation TSD was purchased and commenced data collection operations within Australia and New Zealand (Figure 1). The updated system uses seven Doppler lasers located 100 mm, 200 mm, 300 mm, 450 mm, 600 mm, 900 mm and 3500 mm ahead of the loaded rear wheel. In addition, several other technologies were integrated within the TSD upon arrival to Australia from the ARRB Group's Hawkeye suite. These included automated crack detection, environmental cameras, texture and roughness lasers and pavement temperature sensors. To validate the analysis approach tested previously by Muller & Roberts [6] on the updated TSD equipment, several field investigations were undertaken showing repeatable d_0 results that compared well with FWD measurements [11]. Here TSD d_0 refers to the deflection estimate at zero offset from the centre of the wheel load, which may differ from the maximum deflection when a lag occurs between the passage of the loaded wheel and the resulting pavement response. This differs from FWD, where the maximum deflection and deflection at zero offset are the same. After initial commissioning and validation of the updated TSD device, data collection began in earnest from April 2014. As at March 2015, more than 40,000 km of data have been collected within Queensland, New South Wales and New Zealand.

Figure 1: Second-generation TSD device

2.2 Noise-Modulated Ground Penetrating Radar

Noise-Modulated Ground Penetrating Radar (NM-GPR) is a GPR variant using coded signal modulation and efficient receiver hardware to enable traffic-speed multi-channel performance [12-15]. Developed in Australia by Radar Portal Systems, the first generation of NM-GPR technology has been used for a range of road investigations for the Queensland Department of Transport and Main Roads (TMR) since 2008 [4]. The technology has been recently updated to improve measurement sensitivity [12] and achieve multi-offset operation, providing potential for calibrated road layer depth measurements and quantitative moisture mapping applications [16, 17]. Unlike other GPR systems, this equipment uses multiple dedicated

hardware receivers combined with an array of ground coupled antennas and custom damping systems in a trailer format to collect 3D data while travelling at speeds of up to 100 km/h. The equipment used for this investigation is shown in Figure 2. Recent testing of a half-width trailer version of this technology in Japan demonstrated compliance with US Federal Communications Commission (FCC) limits.

Figure 2: Second-generation traffic-speed 3D NM-GPR trailer.

2. Field investigation

2.1 Site selection

Between April and August 2014 approximately 10,000 km of TSD data were collected on state-controlled roads within Queensland, providing a large number of potential sites for comparison with FWD and NM-GPR. To minimise investigation costs, five sites were selected where FWD testing had already been undertaken on the same road and close to the date of the TSD investigation. All of the locations investigated with FWD were granular pavements that had previously been rehabilitated using foamed bitumen stabilisation. The presented FWD d_0 data are 40 kN measurements scaled linearly up to 50 kN, to bring it closer to the load applied by TSD. The NM-GPR data were collected approximately one year after the 2014 FWD and TSD testing and were analysed using the approach outlined in [6] and [11]. Two of the sites were then re-scanned with TSD in 2015, approximately one year after the initial scan. For those sites scanned twice, the NM-GPR data were collected on the same day as the latter TSD scan.

2.2 Geospatial displays and automated alignment

As a simple, visual means of viewing and comparing data, a geospatial display of TSD, FWD and NM-GPR measurements was developed using Google Earth™ software. The global navigation satellite system (GNSS) measurements collected by each device were used to locate the measurements, inspired by data display examples from other fields [18]. An automated means of aligning data to the state government chainage system was also developed. Examples using this approach are presented in Figures 3 to 7. In these figures the TSD d_0 results are

illustrated as vertical bars, the colour and height of which are proportional to the deflection magnitude. The FWD d_0 results are illustrated as white markers, to the same scale as the TSD. Both TSD and FWD results are illustrated on top of the NM-GPR data, shown as a continuous geo-located 'radargram' image. This approach provides a quick and simple comparison of the pavement structure and the resulting deflection response without having to first interpret GPR layer interfaces. The horizontal scale lines shown in Figures 3 to 7 represent increments of 0.2mm for the deflection data and 200 mm increments of depth for the NM-GPR data, assuming a relative permittivity of 5 for the pavement materials.

2.3 Results

2.3.1 Boonah-Beaudesert Road

The TSD data were collected on the Boonah-Beaudesert Road on 1 May 2014. The FWD testing was undertaken on 19 May 2014, measuring at 25m intervals from chainage 3.2 to 4.1 km, coinciding with the extent of the foam bitumen treatment. The NM-GPR data were collected approximately one year later, on 14 April 2015. The geolocated data are illustrated in Figure 3.

As shown in this figure, a similar trend in the TSD and FWD d_0 results can be seen over the length of FWD testing, the values of which are generally less than 0.2 mm. A distinct change can be seen in the NM-GPR at chainage 4.0 km, coinciding with the end of the stabilisation, though the start of stabilisation is less clear in the data. A change in the NM-GPR response at approximately 3.35 km appears to be due to a variation in the pavement coupling with the ground coupled antennas. Various other changes in pavement structure can also be seen in the NM-GPR data, some of which also coincide with changes in the TSD response and features in the geospatial imagery. An example of this is between chainage 2.5 to 2.6 km, where the TSD reports invalid results. Here, the NM-GPR response shows a five-cell culvert and the geospatial imagery show a watercourse. Thus, in this instance the NM-GPR response and geospatial data can enable a better understanding of the reasons for the TSD response.

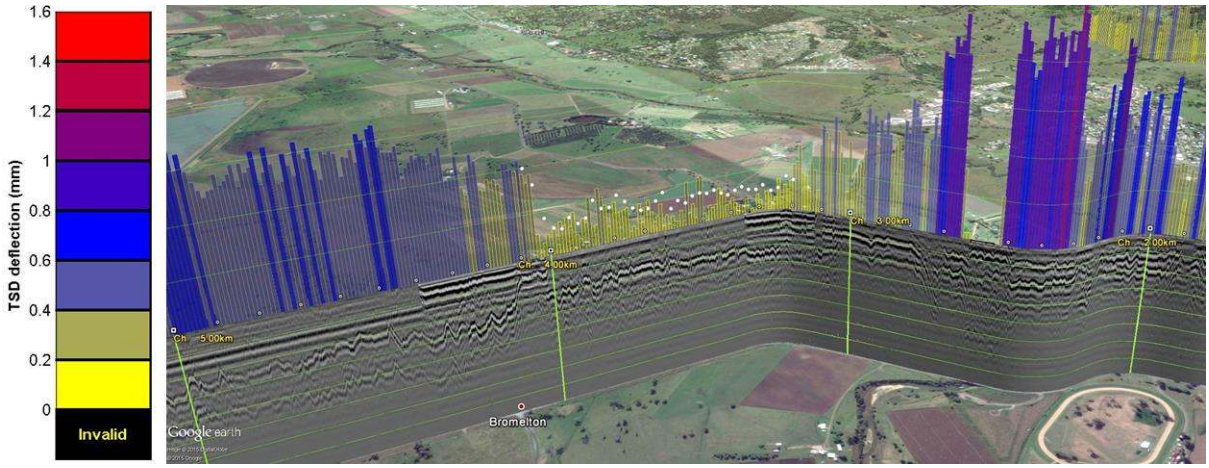

Figure 3: Boonah-Beaudesert Road, chainage 1.9 to 5.0 km showing a geospatial display of outer wheel path TSD d_0 (coloured bars), a continuous greyscale NM-GPR radargram and FWD d_0 values (white markers) Source: Google Earth™, "map title, scale" map data; Image: Digital Globe, Google.

2.3.2 Mount Lindsay Highway

FWD testing for this road was undertaken on 20 May 2014 at 25 m intervals between chainage 11.5 to 13.5 km. The TSD investigation for this road was undertaken on 1 May 2014, 19 days prior to the FWD investigation. The NM-GPR for this site was collected approximately one year later, on 14 April 2015.

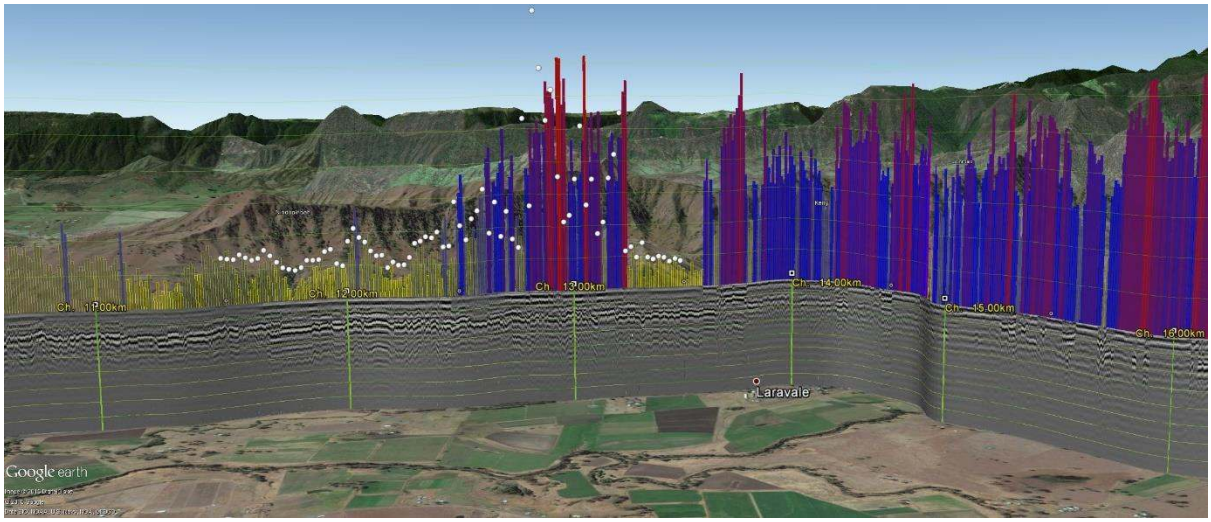

Figure 4: Mt Lindsay Highway, approximate chainages 10.6 to 16.1 km illustrating TSD d_0, NM-GPR and FWD d_0 data.
Source: Google Earth™, "map title, scale" map data; Image: DigitalGlobe, Data SIO, NOAA, U.S. Navy, NGA, GEBCO, Google.

A similar pattern in the FWD and TSD d_0 values is observed, though with some variations in the results, particularly in the region of the higher deflection result from chainage 12.5 to 13.2 km. The NM-GPR data indicate a relatively consistent total pavement depth over the length tested by FWD, though both TSD and FWD results vary from less than 0.2 mm to more than 1.4 mm over this length. A number of features in the NM-GPR data appear to align with changes in the TSD data, for example the change in construction from chainage 13.65 to 13.9 km corresponding with increased deflection results and isolated patches between chainage 15.3 to 15.9 km corresponding to variations in the magnitude of TSD d_0 results.

2.3.3 Stayplton - Jacobs Well Road

FWD testing for this site was undertaken on 16 May 2014 at 25 m intervals from chainage 11.5 to 13.5 km. The TSD investigation was undertaken on 24 April 2014 and the NM-GPR data were collected on 14 April 2015. Over the length of FWD testing there is good agreement in the pattern of TSD and FWD d_0 results which are also relatively consistent and coincide with a change of construction in the upper 400 mm of pavement visible in the NM-GPR response, presumably the stabilisation repair. Either side of this section the pavement depth appears approximately 200 to 250 mm deep, coinciding with a notable increase in the TSD d_0 results.

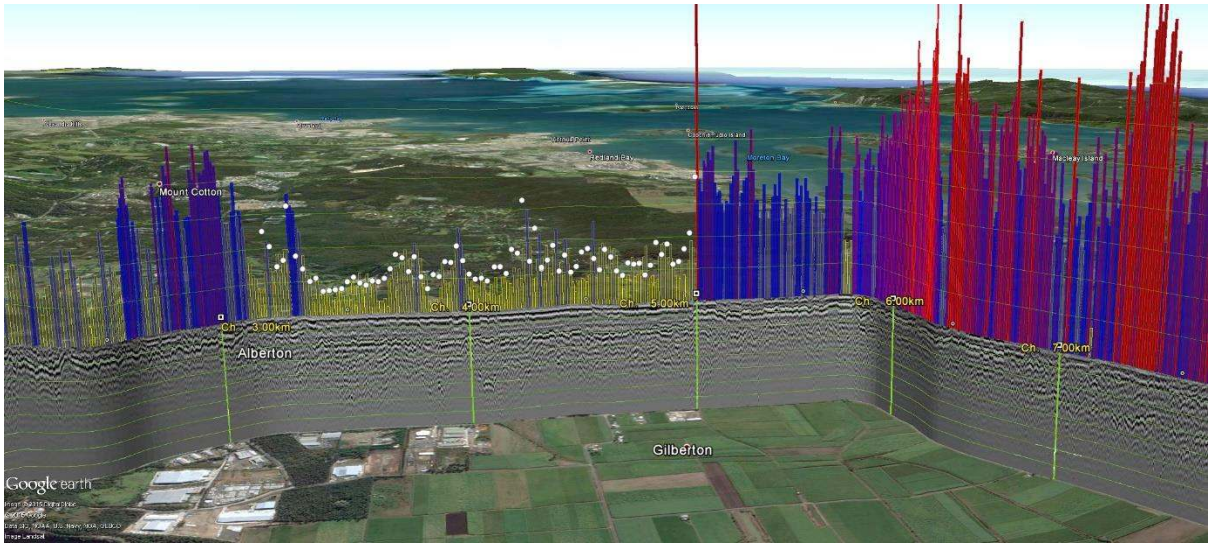

Figure 5: Stayplton – Jacobs Well Road, chainage 2.1 – 7.6 km showing a geospatial display of outer wheel path TSD d_0, NM-GPR and FWD d_0 data.
Source: Google Earth™, "map title, scale" map data; Image: DigitalGlobe, Data SIO, NOAA, U.S. Navy, NGA, GEBCO, Landsat, Google.

2.3.4 New England highway

FWD testing on the New England Highway was undertaken at 25 m intervals for two locations, location 1 from chainage 34.4 to 35.4 km tested on 1 April 2014 (Figure 6) and location 2 from chainage 54.7 to 55.7 km tested on 31 March 2014 (Figure 7). The two TSD runs for these sites were collected almost exactly one year apart, on 23 April 2014 and on 24 April 2015. The NM-GPR data were collected the same day as the later TSD investigation.

Considering location 1, the pattern of 2014 FWD results are similar to the TSD measurements collected in 2014 (Figure 6(a)) and in 2015 (Figure 6(b)), with both methods indicating increased deflection results at approximately chainage 34.8 km and from 35.1 to 35.2 km. These features appear to coincide with near-surface reflections in the NM-GPR response, though the total pavement thickness appears relatively consistent over the length shown in Figure 6.

For location 2, the TSD d_0 results from 2014 and 2015 and the 2014 FWD d_0 results again show a similar overall pattern, though the magnitude of the deflection results varies to a greater extent than for location 1. The NM-GPR results also reflect this site variability, with numerous subsurface features visible at approximately 200 to 400 mm depth from the surface, which may in turn provide clues as to the causes and possible remediation of associated defects or deterioration mechanisms.

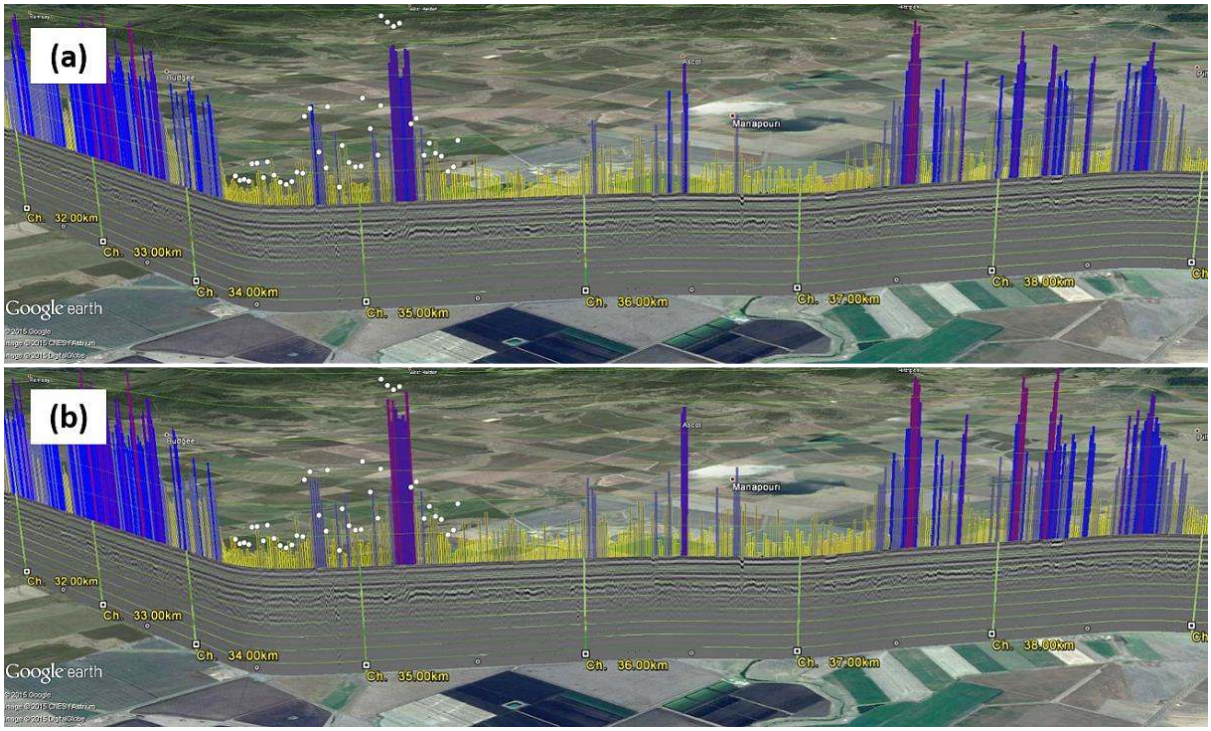

Figure 6: New England Highway, location 1 comparing FWD d_0 data collected 31 March 2014, NM-GPR data collected 24 April 2015 and TSD d_0 data collected (a) 23 April 2014 and (b) 24 April 2015.
Source: Google Earth™, "map title, scale" map data; Image: CNES / Astrium, Digital Globe, Google.

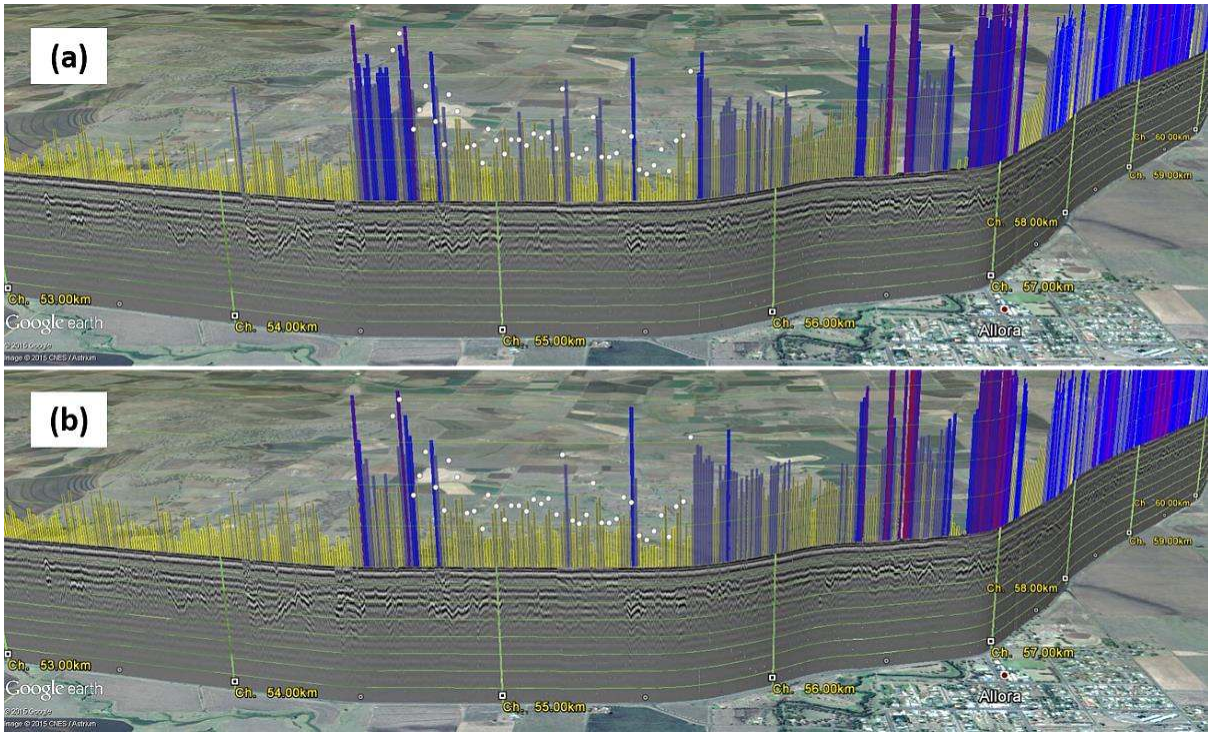

Figure 7: New England Highway, location 2 comparing FWD data collected 1 April 2014, NM-GPR data collected 24 April 2015 and TSD data collected (a) 23 April 2014 and (b) 24 April 2015.
Source: Google Earth™, "map title, scale" map data; Image: CNES / Astrium, Google.

3. Discussion

Several general observations can be made based on the TSD, FWD and NM-GPR data presented in Figures 3 to 7:

1. Overall the pattern of TSD d_0 and 40 kN FWD d_0 measurements scaled to 50 kN appear similar in shape and magnitude, though with some variation in places.
2. In some locations, changes noted in the NM-GPR data correspond with changes in the TSD and FWD response. This correlation in turn implies probable causation. That is, the change in subsurface features has most likely led to the variation in the measured deflection response. For example, where a variation in the pattern of deflection results coincides with a construction change, a feature such as a culvert, or subsurface defects.
3. In other locations, changes within the TSD and FWD response do not correspond with changes in the NM-GPR response, indicating a different type of explanation. For example, where the NM-GPR reports a relatively consistent pavement layering but the deflection magnitude varies, which may in turn be due to degradation of the strength of a pavement layer.
4. The magnitude and pattern of TSD results collected one year apart, illustrated in Figures 6 and 7, are relatively consistent. This may indicate consistency of the pavement response and TSD measurements over this period, though it is unclear if the deflection results varied between the measurement dates.
5. The use of geospatial imagery is helpful in understanding how the surrounding environment has affected the TSD, FWD and/or NM-GPR response. For example, features such as watercourses, topography or the presence of industrial activities (e.g. nearby quarries, farms) can be used to provide clues as to the factors affecting road demand and performance.

The examples given in Figure 3 to 7 illustrate a simple method of viewing TSD and FWD d_0 results with NM-GPR and environmental imagery to identify patterns in pavement structure and better understand the underlying causes of pavement response. Moving on from mere visual comparisons, the next step is to consider back-analysis of the TSD bowls collected on flexible pavements using NM-GPR to determine or confirm layer depths, analogous to the conventional combination of FWD and GPR [19, 20]. Here the development of automated methods of calibrating GPR layer depth estimates, for example using multi-offset GPR methods [17], becomes important as accurate layer depths are important in the back-analysis of layer moduli [21, 22]. Like the combination of FWD and GPR, the combined use of TSD and GPR provides independent measurements covering different aspects of the pavement response. Such an approach reduces the risk of misinterpreting the causes of pavement distress based on incomplete or ambiguous results from only one device. For example, two pavements with a different thickness or configuration may be correctly differentiated by GPR, however if they have a similar deflection response they may not be discernible using TSD or FWD. Conversely, GPR may indicate a relatively consistent pavement layering in places where the deflection response varies due to localised degradation or other material changes.

4. Conclusions

A comparison of second-generation TSD, NM-GPR and conventional FWD was undertaken for five test locations within Queensland, Australia. The measurements were displayed geospatially using Google Earth™ software and comparisons were undertaken at selected locations based on visual observations.

Overall there was a clear correlation in the pattern and magnitude of TSD and FWD results for all sites; and TSD results for the two sites tested a year apart showed very similar results. In places, changes in pavement structure, the presence of buried infrastructure or subsurface anomalies observed in the NM-GPR response coincided with changes in the TSD and FWD response, indicating a likely cause or contributor to the deflection response. In other locations the NM-GPR revealed relatively homogenous pavement layering where the TSD and FWD indicated significant variation, indicating the change in deflection is unrelated to the consistency of the pavement structure. Such observations at the five test sites indicate the independent and complementary nature of TSD and GPR measurements. The combined use of TSD and NM-GPR, preferably collected simultaneously, is therefore recommended for rapid non-destructive assessments of flexible pavements.

Acknowledgements

This work was funded under the National Asset Centre of Excellence (NACOE) program of research undertaken for the Department of Transport and Main Roads by the ARRB Group Ltd. This work contributes to and supports the work of COST Action TU1208 ‘Civil Engineering Applications of Ground Penetrating Radar’.

References

[1] J. Kelley and M. Moffat, "Review of the Traffic Speed Deflectometer - Final Project Report," ARRB Group, Melbourne, Australia, Austroads Report AT1613, 2011.

[2] S. Baltzer, D. Pratt, J. Weligamage, J. Adamsen, and G. Hildebrand, "Continuous bearing capacity profile of 18,000km Australian road network in 5 months," in 24th ARRB Conference, Melbourne, Australia, 2010.

[3] B. W. Ferne, P. Langdale, N. Round, and R. Fairclough, "Development of the UK highways agency traffic speed deflectometer," in Bearing Capacity of Roads, Railways and Airfields, E. Tutumluer and I. L. Al-Qadi, Eds., ed Champaign, Illinois, USA: Taylor & Francis Group, London UK, 2009, pp. 409-418.

[4] W. B. Muller, "A network-level road investigation trial using Australian-made traffic-speed 3D Ground Penetrating Radar (GPR) technology," in 25th ARRB Conference, Perth, Western Australia, Australia, 2012.

[5] W. Muller and B. Reeves, "Comparing Traffic Speed Deflectometer and Noise-Modulated Ground Penetrating Radar data for rapid road pavement investigations," in 14th International Conference on Ground Penetrating Radar (GPR-2012), Shanghai, China, 2012, pp. 502-509.

[6] W. B. Muller and J. Roberts, "Revised approach to assessing Traffic Speed Deflectometer (TSD) data and field validation of deflection bowl predictions," International Journal of Pavement Engineering, vol. 14, no. 4, pp. 388–402, 2013

[7] J. Krarup, S. Rasmussen, L. Aagaard, and P. G. Hjorth, "Output from the Greenwood Traffic Speed Deflectometer," in 22nd ARRB Conference, Canberra, Australia, 2006.

[8] L. Pedersen, "Viscoelastic Modelling of Road Deflections for use with the Traffic Speed Deflectometer," Doctor of Philosophy thesis, Department of Mathematics, Technical University of Denmark, 2012.

[9] A. Zofka, J. Sudyka, M. Maliszewski, P. Harasim, and D. Sybilski, "Alternative Approach for Interpreting Traffic Speed Deflectometer Results," Transportation Research Record: Journal of the Transportation Research Board, vol. 2457, pp. 12-18, 2014.

[10] N. Piyatrapoomi, L. Gunapala, and J. Weligamage.). Traffic Speed Deflectometer (TSD): Queensland Trial. Queensland Roads, ed. 9., pp. 16-27, Dept. of Transport and Main Roads, Queensland, Australia, 2010.

[11] W. Muller and R. Wix, "Preliminary field validation of the updated Traffic Speed Deflectometer (TSD) device," in 26th ARRB Conference, Sydney, Australia, 2014.

[12] B. Reeves, "Noise modulated GPR: Second generation technology," in 15th International Conference on Ground Penetrating Radar (GPR-2014), Brussels, Belgium, 2014, pp. 708-713.

[13] B. Reeves, "Automatic Road Surface Assessment and High Speed 3D GPR Technology," in NDE/NDT for Highways and Bridges, Structural Materials Technology (SMT), New York City, NY, USA, 2010, pp. 326-333.

[14] W. B. Muller and B. Reeves, "Application of a traffic-speed road scanning system including a new type of 3D GPR," in NDE/NDT for Highways and Bridges, Structural Materials Technology (SMT), New York City, NY, USA, 2010, pp. 538-545.

[15] B. Reeves and W. Muller, "Traffic-speed 3-D Noise Modulated Ground Penetrating Radar (NM-GPR)," in 14th International conference on Ground Penetrating Radar (GPR-2012), Shanghai, China, 2012, pp. 165-171.

[16] W. B. Muller, A. Scheuermann, and B. Reeves, "Quantitative moisture measurement of road pavements using 3D GPR," in 14th International Conference on Ground Penetrating Radar (GPR-2012), Shanghai, China, 2012, pp. 517-523.

[17] W. Muller, "Self-correcting pavement layer depth estimates using 3D multi-offset ground penetrating radar (GPR)," in 15th International Conference on Ground Penetrating Radar (GPR-2014), Brussels, Belgium, 2014, pp. 887-892.

[18] A. Chen, G. Leptoukh, S. Kempler, C. Lynnes, A. Savtchenko, D. Nadeau, et al., "Visualization of A-Train vertical profiles using Google Earth," Computers and Geosciences, vol. 35, pp. 419-427, 2009.

[19] T. Saarenketo, "Chapter 13 - NDT Transportation," Ground Penetrating Radar Theory and Applications, M. J. Harry, Ed., Elsevier, 2009, pp. 393-444.

[20] T. Scullion and T. Saarenketo, “Integrating ground penetrating radar and falling weight deflectometer technologies in pavement evaluation”, Nondestructive Testing of Pavements and Backcalculation of Moduli: Third Volume, ASTM STP 1375, S. D. Tayabji and E. O. Lukanen, Eds., American Society for Testing and Materials, West Conshohocken, PA, USA, 2000, pp. 23-37

[21] L. H. Irwin, W. S. Yang, and R. N. Stubstad, “Deflection reading accuracy and layer thickness accuracy in backcalculation of pavement layer moduli”, Nondestructive testing of pavements and backcaulation of moduli, ASTM STP 1026, A. J. Bush III and G. Y. Baladi, Eds., American Society for Testing and Materials (ASTM), Philadelphia, 1989, pp. 229-244.

[22] M. Ahmed, R. Tarefder, and A. Maji, "Variation of FWD modulus due to incorporation of GPR predicted layer thicknesses," in 15th International Conference on Ground Penetrating Radar (GPR-2014), Brussels, Belgium, 2014, pp. 345-350.